

Motor cortex excitability states in chronic stroke patients probed by EEG-TMS



Arianna Brancaccio ^{a, id}, Davide Tabarelli ^a, David Baur ^{b,c, id}, Johanna Roesch ^{b,c}, Wala Mahmoud ^{b,c}, Ulf Ziemann ^{b,c,* id}, Paolo Belardinelli ^{a,b,c}

^a Center for Mind/Brain Sciences—CIMeC, University of Trento I-38123 Trento, Italy

^b Department of Neurology & Stroke, University of Tübingen, Germany

^c Hertie-Institute for Clinical Brain Research, University of Tübingen, Germany

ARTICLE INFO

Keywords:

Stroke
Motor cortex
Cortical excitability
Transcranial magnetic stimulation
TMS-EEG

ABSTRACT

Objective: In healthy subjects, the trough vs. no-trough phases of the sensorimotor μ -rhythm correspond to high- vs. low-excitability states of the motor cortex (M1). We tested this excitability differentiation in the ipsilesional (iM1) and contralateral M1 (cM1) of chronic stroke patients.

Methods: 19 chronic stroke patients received single-pulse transcranial magnetic stimulation (TMS), separately over the iM1 and cM1, during EEG recordings. High and low M1 excitability states were defined by binning a post-hoc estimate of the μ -phase at TMS delivery. TMS-evoked EEG potentials (TEPs) and time-frequency responses were characterized for excitability states and hemispheres. The motor function of the affected arm was tested by the Fugl-Meyer Assessment Upper Extremity (FMA-UE).

Results: In cM1, TMS at the high- vs. low-excitability state resulted in larger TEP amplitudes and increased post-pulse power in the beta band. In iM1, these modulations were not significant except for post-pulse beta power. This retained excitability differentiation significantly correlated with FMA-UE.

Conclusions: The degree of excitability differentiation in iM1 depending on phase of the sensorimotor μ -rhythm correlates with individual affected upper extremity motor function.

Significance: The degree of excitability differentiation in iM1 might serve as a new independent marker of motor recovery.

1. Introduction

The worldwide incidence of stroke has been rising over the recent decades (Brainin et al., 2007, Katan and Luft, 2018) and stroke is the global leading cause for sustained severe motor disability. Previous studies demonstrated that the complexity of transcranial magnetic stimulation (TMS)-evoked EEG responses over the motor cortex (M1) is associated with alterations in corticospinal excitability resulting from lesions that impact motor function. In particular, the complexity of TMS-evoked EEG responses over M1 correlates with changes in cortico-spinal excitability. Casula et al. showed a reduced cortical evoked EEG response following single-pulse TMS (spTMS) over M1 in the ipsilesional M1 compared to both contralateral hemisphere and the healthy brain (Casula et al., 2021). Conversely, five other studies (Harquel et al., 2022, Sarasso et al., 2020, Tecchio et al., 2023, Tscherpel et al., 2020;

Tscherpel et al., 2024) found low-complexity, high-amplitude biphasic EEG responses to spTMS of ipsilesional M1 (iM1), in particular in severely affected patients. We here draw on findings from brain state-dependent stimulation experiments in healthy subjects. Real-time EEG-TMS 1) shows modulation of motor-evoked potential (MEP) amplitudes with phase of the ongoing sensorimotor μ -rhythm (Wischnewski et al., 2022, Zrenner et al., 2018) and 2) reduces inter-individual variability in plasticity effects induced by repetitive TMS (rTMS) (Baur et al., 2020, Zrenner et al., 2018). Zrenner and colleagues report two relevant findings on corticospinal excitability and plasticity, both determined by the instantaneous phase of the sensorimotor μ -oscillation at the time of stimulation (Zrenner et al., 2018). MEPs are systematically larger in amplitude when the TMS pulse is released over M1 at the negative peak (trough) of the sensorimotor μ -rhythm compared to other phases. Secondly, high-frequency rTMS triplets applied over M1 consistently at the

* Corresponding author at: Hertie-Zentrum für Neurologie, Hertie-Institut für klinische Hirnforschung Abteilung Neurologie mit Schwerpunkt neurovaskuläre Erkrankungen, Hoppe-Seyler-Str., 372076 Tübingen, Germany.

E-mail address: ulf.ziemann@uni-tuebingen.de (U. Ziemann).

trough of the μ -rhythm (i.e., the high excitability state of the corticospinal system) induced a long-term potentiation-like increase in MEP amplitude, while the same stimulation at the positive peak of the μ -rhythm induced nil effects, no different from random phase stimulation (Zrenner et al., 2018). The relevance of the μ -oscillation phase on rTMS-induced M1 plasticity was confirmed by Baur et al. who found that low-frequency rTMS applied consistently at the positive peak (i.e., the low-excitability state) induced a long-term depression-like decrease in MEP amplitude (Baur et al., 2020). Differently, the same intervention synchronized with the μ -oscillation *trough* induced a trend towards long-term potentiation. In summary, the brain state (here, the excitability state of the corticospinal system proxied by the phase of the sensorimotor μ -rhythm) determines to a significant extent the magnitude and direction of plasticity induction by non-invasive brain stimulation.

Here, we analyzed TMS-EEG data in a cohort of moderate-to-severely impaired chronic stroke patients. A subgroup of these patients received spTMS only over the M1 of the IH, while the other patients received spTMS of both IH and CH. We applied offline post-hoc phase-bin sorting based on the phase of the μ -oscillation recorded over iM1 and contralateral M1 (cM1) at the time of spTMS. In this regard, it is worth noticing that Hussain et al. provided evidence of the feasibility of accurate μ -phase detection in the ipsilesional M1 of chronic stroke patients (Hussain et al., 2020).

We aimed at estimating the effect of sensorimotor μ -oscillation phase on TMS-EEG excitability metrics in the iM1 and cM1 of chronic stroke patients, with the following overarching hypothesis: despite preserved presence of the μ -rhythm in the iM1, the neurobiological function of this rhythm with regard to corticospinal excitability is reduced or even absent. The phase-state effects on TMS-EEG signals were assessed by time domain TMS-evoked potentials (TEPs) and time-frequency responses (TFRs). Through these metrics we investigated whether spTMS at the *trough* (i.e., the high excitability state) vs. all other phases of the μ -rhythm (i.e., the low excitability state) provided different effects in the iM1 vs. cM1 (Experiment 1).

TEPs have been proposed as a possible proxy of the excitatory/inhibitory balance of the human cortex. Pharmacological-TMS-EEG studies showed that GABAergic and anti-glutamatergic drugs increase the amplitude of the N45 TEP-component (Belardinelli et al., 2021; Premoli et al., 2014), while a GABA-R antagonist attenuated this response (Darmani et al., 2016). Moreover, Casula et al. showed that low-frequency rTMS increases the amplitude of the P70 and N100 TEP components and concluded that these TEP components reflect inhibitory processes (Casula et al., 2014). These findings support the notion that TEPs reflect excitation/inhibition balance in human cortex. Desideri and colleagues have investigated TEPs by sorting them on the basis of the μ -phase at the time of the TMS pulse in healthy participants (Desideri et al., 2018; Desideri et al., 2019). They reported brain state-dependent modulation of TEPs to spTMS but no significant plasticity effect due to phase-dependent rTMS. SpTMS at the *trough* of the sensorimotor μ -rhythm led to a larger amplitude of the P70 and N100 components compared to stimulation at the positive μ -alpha peak. For these reasons, TEPs were proposed as proxies of cortical excitability, as spTMS at the μ -*trough* activates a larger neuronal population than stimulation at the positive peak (Desideri et al., 2019). Based on previous results (Sarasso et al., 2020; Tecchio et al., 2023; Tscherpel et al., 2020; Tscherpel et al., 2024), we expected to find a high-amplitude and low-complexity TMS-evoked EEG response with stimulation of the ipsilesional M1 in our sample of moderate-to-severely affected patients.

We also computed the TFRs from EEG activity in both the IH and CH as a function of the targeted local μ -rhythm phase-state. Alpha and beta power changes following single-pulse TMS (spTMS) have been found in healthy participants (Fecchio et al., 2017; Manganotti et al., 2012) and also a modulation of the same rhythms due to rTMS and continuous theta bursts (cTMS) interventions has been repeatedly reported (Chung et al., 2015; Veniero et al., 2011; Vernet et al., 2013). In particular, Veniero et al. showed that spTMS-induced alpha power increases after

high-frequency rTMS of M1, suggesting that this metric reflects the sensorimotor excitability state (Veniero et al., 2011). Starting from these results, we specifically hypothesize spTMS-induced alpha and beta power to be selectively modulated by the phase of the μ -rhythm at the time of spTMS of the cM1 but not or to a lesser extent with spTMS of the iM1.

The effects of the μ -oscillation phase on the above-mentioned metrics have been investigated in the main analysis (denoted as Experiment 1). In a second analysis (Experiment 2), we investigated the interplay between the degree of differentiation of the two excitability states and the level of impairment, as measured with the individual Fugl-Meyer Assessment Upper Extremity (FMA-UE) score (Fugl-Meyer et al., 1975). In Experiment 1) the unique metric showing a significant dependence on the μ -oscillation phase at time of stimulation of iM1 and cM1 was the TMS-induced beta power. Considering also that beta power has been shown to correlate with the level of motor performance in stroke patients (e.g., (Foong et al., 2019; Wu et al., 2016)), we defined a μ -oscillation phase dependent post-pulse beta power index and hypothesized it to be correlated with the individual FMA-UE. Moreover, we computed the perturbational complexity index (PCI) (Casali et al., 2013; Comolatti et al., 2019) with different electrodes selections, to assess how our index performs compared to this metric, specifically designed to assess TMS-induced perturbation complexity in EEG signals.

2. Materials and methods

2.1. Participants

Recruitment and Experiments were conducted at the University of Tübingen, Germany, at the Department of Neurology and Stroke, and the Hertie Institute for Clinical Brain Research. Experiments were executed in accordance with the Declaration of Helsinki and were approved by the local ethics committee of the medical faculty of the University of Tübingen (530/2019BO1). All participants provided written informed consent before the start of the measurements. TMS-EEG measurements in stroke patients were performed during the screening session of a TMS therapy study (ClinicalTrials.gov ID: NCT05005780). Inclusion criteria were defined as follows: 1) chronic stroke ≥ 6 months post-stroke; 2) age between 18 and 85 years; 3) persistent upper extremity motor impairment due to stroke with a Fugl-Meyer Assessment Upper Extremity (FMA-UE) score < 60 ; 4) preserved MEPs $\geq 50 \mu\text{V}$ in the first dorsal interosseous (FDI) of the affected hand by TMS of iM1. Patients were excluded if they fulfilled at least one of the following criteria: 1) history of epileptic seizures; 2) intracranial or cardiac implants or any other metal objects located in ≤ 10 cm distance to the TMS coil (excluding the mouth); 3) intake of proconvulsive or muscle-relaxing medication; 4) inability to follow the study instructions or provide informed consent; 5) pregnancy or intention to become pregnant. Of the initially 79 patients screened, 26 patients fulfilled these criteria. Because of low signal-to-noise (SNR) of the sensorimotor μ -oscillation, data from 7 stroke patients had to be discarded. Furthermore, since our experimental conditions depended on a post-hoc determination of the μ -oscillation phase at the time of TMS, the number of trials in a given condition was a variable fraction of the overall number of trials available for the individual patient. For this reason, not all of the 19 patients who, according to Table, were eligible for at least one of the two experiments performed in this work, was included. The inclusion criterion was a total number of trials larger than 50 for each of the two phase conditions (*trough*, *no-trough*). Moreover, in Experiment 1, only the patients who received stimulation of both CH and IH were included, while in Experiment 2 only patients for which the FMA-UE was available were included. This led to a total of 12 patients for Experiment 1 and 17 patients in Experiment 2. Demographic and lesion characteristics of the final stroke sample are shown in Table 1. FMA-UE scoring was performed by a qualified rater that was blinded to all other patient characteristics. Supplementary Table 1 reports further details on the

Table 1

Characteristics of the stroke patient dataset. Other than demographic information (gender and age) the time post-stroke (TPS), Fugl-Meyer Assessment Upper Extremity score (FMA-UE) as well as site/hemisphere and type of lesion are reported. The column “Experiment” indicates in which analysis subjects were included, depending on available data. The last column indicates the available MRI sequences on which the individual lesion volume was segmented for producing the lesion overlap map across patients in Fig. 1 (T1w-HR and T1w refer to research high-resolution scans and clinical scans, respectively). At the bottom, means and standard deviations (SD) are reported. NA, not available. EXP, Experiment The maximum possible value for the FMA-UE score is 66, indicating no impairment of motor function.

PATIENT	AGE (years)	SEX	LESION			TPS (months)	FMA-UE	EXP	MRI
			Lesion location	Hemisphere	Type				
S1	62	M	subcortical	left	hemorrhagic	16	22	1 + 2	T1w
S2	51	F	cortical + subcortical	right	ischemic	97	49	1 + 2	T1w -HR
S3	60	M	cortical + subcortical	left	ischemic	22	NA	1	T1w
S4	79	F	no MRI	right	ischemic	13	NA	1	NA
S5	62	M	cortical + subcortical	left	ischemic	66	30	1 + 2	T1w
S6	61	M	subcortical	right	ischemic	35	41	1 + 2	T1w
S7	66	M	subcortical	left	ischemic	36	34	1 + 2	T2w
S8	57	F	no MRI	right	hemorrhagic	24	59	1 + 2	NA
S9	69	M	cortical + subcortical	right	hemorrhagic	126	19	1 + 2	T2w
S10	53	F	cortical + subcortical	right	hemorrhagic	148	16	1 + 2	T1w-HR
S11	72	M	cortical + subcortical	right	ischemic	36	57	2	T1w
S12	67	M	subcortical	right	ischemic	50	32	2	T1w
S13	39	M	subcortical	left	ischemic	12	38	2	T1w
S14	53	M	no MRI	right	ischemic	29	45	2	NA
S15	59	M	subcortical	left	ischemic	27	56	1 + 2	T1w-HR
S16	44	F	cortical + subcortical	left	ischemic	12	59	1 + 2	T1w-HR
S17	54	M	cortical + subcortical	right	ischemic	180	58	1 + 2	T1w-HR
S18	70	M	cortical + subcortical	left	ischemic	120	39	1 + 2	T1w
S19	62	M	cortical + subcortical	right	ischemic	12	60	1 + 2	T1w-HR
Means ± SD	60 ± 10	F = 5				56 ± 52	42 ± 15		

number of trials in each included patient.

2.2. TMS-EEG recordings

Experiments were performed in accordance with current safety guidelines (Rossi et al., 2021). Participants were seated on a comfortable chair for the whole duration of the TMS-EEG experiment. EMG was recorded by surface electrodes (Kendall, Covidien, Ireland) in a bipolar belly-tendon montage from the first dorsal interosseus (FDI) muscle contralateral to the stimulated hemisphere. A 64-channel Ag/AgCl sintered ring electrode cap (EasyCap GmbH, Germany) with a dense electrode arrangement over the sensorimotor cortex (for details see Supplementary Fig. 1) was used for EEG registration. Electrodes were prepared by mild skin abrasion and filled by a conductive gel (Electrode Cream, GE Medical Systems, USA) until the desired impedance of $<5\text{ k}\Omega$ was attained. EEG and EMG were recorded simultaneously with a 24-bit biosignal amplifier (NeurOne Tesla with Digital Out Option, Bittium Biosignals Ltd., Finland) at a sample rate of 5 kHz. Head position was stabilized by a vacuum pillow around the neck (Vacuform, B. u. W. Schmidt GmbH, Germany). Biphasic TMS pulses were delivered by a stimulator (MagPro R30, MagVenture, Denmark) connected to a 75 mm coil (MCF-B65, MagVenture, Denmark). A 5-min eyes open resting-state EEG was recorded after cap preparation. Then, the motor hot spot was identified as the coil position and orientation resulting in highest and most consistent MEP amplitudes in the contralateral FDI, and resting motor threshold (RMT) was defined as the lowest stimulation intensity that elicited peak-to-peak MEPs of $\geq 50\text{ }\mu\text{V}$ in at least 5 out of 10 trials (Rossini et al., 2015). As a next step, 600 spTMS with an interstimulus interval (ISI) of 2.5 s (± 0.25 s jitter) were delivered at 115 % of RMT on the iM1 FDI hotspot. The coil was held by a mechanical arm and its position was marked with a pen on the EEG cap. As the measurements were physically demanding for stroke patients, stimulation was stopped in case patients felt exhausted or uncomfortable. This resulted in a varying numbers of pulses between patients. The actual number of trials, which corresponds to the number of pulses delivered minus the trials discarded during the preprocessing stage, is reported in Supplementary Table 1. If patients still felt comfortable, the same procedure was

repeated over the cM1.

2.3. Data preprocessing

Data preprocessing was performed using MATLAB (The Mathworks, Natick, MA, USA) custom code partially based on functions of the open-source toolboxes EEGLAB and TESA (Delorme and Makeig, 2004, Rogasch et al., 2014). EEG recordings were first visually inspected to exclude bad channels and continuous recordings were then epoched between -1.4 s and $+1.6$ s around the TMS pulse. TMS artefacts were removed from each epoch and interpolated between -5 and 20 ms around the pulse (with cubic interpolation on data 50 ms before and after the pulse). Epochs were then visually inspected again to discard bad trials. After that, SOUND algorithm implemented in TESA was used to attenuate each channel's noise level and interpolate previously discarded bad channels (Mutanen et al., 2018). As TESA-SOUND requires a head model to separate genuine EEG from artefactual signal, we used a standard three-layer spherical head model. Data were then high-pass filtered at 0.5 Hz and data from -5 to 40 ms were removed before using the Fast-ICA TESA implementation for ocular artefacts removal. Epoched data were then baseline corrected (-500 to -50 ms). Finally, the SSP-SIR algorithm was used to clean EEG data from TMS-induced muscular artefacts (Mutanen et al., 2016). After this, a stopband of 48–52 Hz and the respective harmonics up to 500 Hz was applied for filtering out the power line noise. Finally, an anti-aliasing filter at 225 Hz was applied before resampling at 500 Hz.

2.4. Data analysis and statistics

All the subsequent analyses were performed using custom Python code, based on NumPy (Harris et al., 2020), SciPy (Virtanen et al., 2020) and MNE-Python (Gramfort et al., 2013) libraries. Electrode positions for the patients with stroke in the right hemisphere were flipped into the left hemisphere in order to be spatially group-consistent.

2.5. Offline phase detection

In order to perform all subsequent phase-dependent analyses, we first computed a post-hoc estimate of the phase at which stimulation occurred in each single trial and hemisphere of interest. The Individual Alpha Frequency (IAF) peak was first detected for each subject. In order to do this we pooled the activity recorded over the channels belonging to the sensory-motor Hjorth filters of both hemispheres (left/*ipsilesional* Hjorth: central electrode C3, surrounding electrodes C1, C5, FC3, CP3; right/*contralesional* Hjorth: central electrode C4, surrounding electrodes C2, C6, FC4, CP4). From the activity of each selected electrode, we computed a Welch spectrum between 5 and 18 Hz, using data from -0.8 to 0.8 s with respect to the TMS pulse. The spectra were then averaged across channels and normalized for the 1/f noise. A peak detection allowed us to define the IAF for each subject. When possible, activity for ipsilesional and contralesional stimulation session of the same subject was pooled in order to improve IAF detection. The spectra for each subject in the alpha band are reported in Supplementary Fig. 2.

The phase at the time of TMS pulse delivery was computed as follow. For each subject and acquisition, data from each trial were transformed to left/right Hjorth and then filtered between +/- 1 Hz around the IAF (Butterworth 4th order IIR filter; two pass zero-phase). Then we cut EEG activity in time retaining only a portion starting from 3 cycles of IAF and -0.05 s before TMS pulse delivery ($t = 0$). An autoregressive model was used to predict the time series of each trial in the interval between $t = -0.05$ and $t = 0.2$ s. In this way we reconstructed the activity around the pulse, that was removed during the pre-processing phase. By computing the instantaneous phase, through an Hilbert transform for each trial, we were then able to obtain, for each trial, a phase value for the μ -rhythm at the time of stimulation, necessary to classify trials.

We defined as *trough* phase a binning of the phase values between 120 and 240 degrees (i.e., $180 \pm 60^\circ$) and as *no-trough* a condition referring to all other phases. The reason we chose this scheme to define phase-dependent conditions is twofold. First, our classification of the trials is based on a post-hoc phase estimation; therefore, the number of trials belonging to a certain condition depends on the number of stimuli delivered (out of a uniformly random distribution (Zrenner et al., 2023)) within a certain phase interval at IAF in the Experimental session. In the selection process, we choose, as a reasonable requirement for a subject to be included, at least 50 trials for each condition of interest (*trough* and *no-trough*). The number of trials for each condition depends on the phase interval (the larger the interval the higher the number of trials) while its variability depends on the total number of trials available for a given subject. Second, there is evidence that the *trough* and closely neighboring phases constitute a high-excitability state, while the low-excitability state is more broadly distributed around the positive peak (Zrenner et al., 2023). In addition, Zrenner et al. showed that the early rising phase rather than the *trough* of the μ -alpha oscillation coincides with the highest excitability state of M1 (Zrenner et al., 2023). Thus, our *trough* condition reasonably overlaps with the early rising phase of the μ -cycle, while still preserving phase symmetry with respect to the center of the trough (180°). Using this classification scheme, considering the limit of at least 50 trials per condition, we were able to include 12 subjects in Experiment 1 and 17 subjects in Experiment 2 (see Table 1). The distribution of phases for each subject are shown in Supplementary Fig. 3. The total number of trials per condition are reported in Supplementary Table 1.

2.6. Experiment 1

In Experiment 1, the 12 patients who received stimulation of both iM1 and cM1 were included (see Table 1).

Here, we investigated how TEP amplitude and post-pulse TFRs in the alpha and beta band depend on the phase of the μ -oscillation in the iM1 and cM1. In this context, we had four conditions of interest, depending on the stimulated hemisphere and targeted IAF phase: cM1 stimulation

at *trough*, cM1 stimulation at *no-trough*, iM1 stimulation at *trough*, iM1 stimulation at *no-trough*. TEPs were computed for each condition between -0.8 and 0.8 s around the TMS pulse. After a normalization, using a baseline period from -0.8 to -0.05 s with respect to the TMS pulse, data were averaged and transformed using a z-score approach with respect to the mean and standard deviation of the data pooled from both phase conditions within one hemisphere. Non-rectified TEPs of the *trough* and *no-trough* conditions were then statistically compared using a permutation non-parametric paired sample *t*-test (Maris and Oostenveld, 2007) within a time interval from 0.02 to 0.25 s with respect to the TMS pulse. We used a cluster approach to correct for multiple comparison. We defined a channel neighbors structure from the distribution of the 64 channels in the cap (minimum number of neighboring channels to form a cluster, $n = 2$). The statistical threshold both for cluster forming and for cluster non-parametric permutation was set to 0.05. The number of permutations M was set to 2048, which corresponds to the number of independent randomizations available with $n = 12$ subjects in a paired sample scheme ($M = 2^{N-1}$). Contrasts of *trough* vs. *no-trough* conditions were computed intra-hemispherically. Finally, we computed the grand average of TEPs for all channels and on the Hjorth filters in the left and right hemisphere (C3, CP3, CP5 for left and C4, CP4, CP6 for right). Grand averages were computed for the two conditions separately (*trough* and *no-trough*) without any post-hoc phase sorting, in order to compare our results with previous literature in stroke patients (Casula et al., 2021, Tscherpel et al., 2020).

Furthermore, TFR analysis was performed for each condition. TFR coefficients were computed between 5 and 45 Hz and between 0.02 and 0.85 s in steps of 0.05 s using a Morlet wavelet approach with FWHM = 0.75 (Tallon-Baudry et al., 1997). TFR statistics between the conditions of interest were run with the same approach as for TEPs, but separately for the two frequency bands of interest: alpha (8 – 12 Hz) and beta (15 – 30 Hz). The TFRs were statistically compared in an interval from 0.02 to 0.85 s with respect to the pulse delivery, with the same channel neighbor's definition, threshold and number of randomization as in the TEPs statistics.

2.7. Experiment 2

In Experiment 2, patients receiving stimulation solely over the iM1 were also included, provided their FMA-UE was available. This led to the inclusion of a total of 17 patients (Table 1). In this analysis, we investigated whether the FMA-UE score was related to the observed degree of differentiation of the TMS-evoked EEG responses between the excitability states in the iM1. In particular, we focused on post-pulse beta power. This analysis was also informed by previous literature that has shown correlations between beta power and level of motor performance in stroke patients (e.g., (Foong et al., 2019, Wu et al., 2016)). However, the differentiation of spTMS-induced beta power between excitability states was never explored before.

The results obtained in Experiment 1 showed that the TFRs comparing post-pulse beta power evoked at *trough* vs. *no-trough* in the iM1 showed a preserved significant difference early after the TMS pulse on a wide range of electrodes. In particular, we found an extended cluster of significant electrodes in comparing the beta (15 – 30 Hz) activity evoked at *trough* vs. *no trough* with iM1 stimulation.

Starting from this result, in order to characterize in a simple way the beta power modulation difference after the pulse in the two phase conditions, we defined a metric β as the ratio between the total power in the beta band (15 – 30 Hz), averaged across all channels and time of interests, in the two conditions. The metrics β , henceforth denoted as *post-pulse beta ratio*, is defined as follows:

$$\beta = \frac{\langle P_{tr.} \rangle_{t,c,f}}{\langle P_{notr.} \rangle_{t,c,f}}$$

where P represent the power at a specific frequency, channel and time,

the subscripts refers to the *trough* (tr) and *no-trough* (no tr) conditions and the brackets subscripts indicate averaging average over times (t), channels (c) and frequencies (f). We computed β starting from a multi-taper spectral estimator P based on Discrete Prolate Spherical Sequences (DPSS), computed from 15 to 30 Hz, in a time interval from 0.02 to 0.25 s from the pulse delivery and using either all available channels or the channels from each Hjorth montage. A linear fit between the individual post-pulse beta ratios and the FMA-UE score was then performed in order to assess if this simple metric correlates with the level of motor function.

We furthermore computed the Perturbational Complexity Index (PCI), a widely used and empirical metrics aiming at measure brain loss/recovery by means of estimating brain perturbational complexity. We computed PCI using the fast PCI ST implementation, following the same analysis pipeline as in (Comolatti et al., 2019). For each subject, data from all EEG channels were band-pass filtered (1–45 Hz) and activity in a response period (from 20 to 250 ms with respect to the TMS pulse) was normalized using a baseline period (from -500 to -50 ms with respect to the TMS pulse). The same response and baseline period were used then for PCI computation, where the percentage of variance accounted for the internal selection of principal components was set to 95 %. We computed the PCI index either selecting only the channels belonging to the Hjorth filters (C3, CP3, CP5 for left and C4, CP4, CP6 for right hemisphere) or by all channels together. Also in this case, we performed a linear fit between the individual PCIs values and the FMA-UE scores. Additionally, we computed the Spearman's rank correlation coefficient between PCI and beta ratio metrics that significantly correlated with FM score, in order to address the question to what extent alterations in iM1 μ -rhythms phase-dependent excitability modulation were simply a consequence of low TEP complexity in the iM1.

3. Results

3.1. Experiment 1 – TEPs without post-hoc sorting

We first inspected the TEPs computed without post-hoc sorting of excitability states (*trough* vs. *no-trough*) recorded from the C3- and C4-Hjorth filters that refer to the ipsilesional and contralateral sensorimotor cortex, respectively. This qualitative inspection highlighted a much larger response in the stimulated and non-stimulated hemispheres with stimulation of the iM1 compared to the cM1 (Fig. 2A–B).

Furthermore, a less complex response was observed with stimulation of the iM1 (Fig. 2A) as compared to stimulation of the cM1 (Fig. 2B), as in (Sarasso et al., 2020; Tscherpel et al., 2020).

3.2. Experiment 1 – TEPs results with post-hoc sorting based on μ -alpha phase detection

In Experiment 1, TEPs following stimulation over iM1 and cM1 were separately investigated with a phase-dependent bin sorting of trials. At a first qualitative inspection, the TEP time-courses evoked by stimulation over iM1 *trough* appears to be more similar in the two phase conditions (Fig. 2C). Differently, TEPs evoked by stimulation over cM1 (Fig. 2D) show different amplitudes and waveforms in the two conditions.

Quantitatively these observed differences have been confirmed by the results of the cluster statistics comparing the EEG activity evoked at the two excitability states of M1 (Fig. 3): stimulation of the cM1 at *trough* elicited significantly larger TEPs in both the stimulated contralateral hemisphere, and in the ipsilesional M1 contralateral to stimulation than stimulation at *no-trough*. Four significant clusters emerge from this contrast at similar time intervals in pair. A first pair of significant clusters (Fig. 3A–B) has occurred in the time interval between 0.02 and 0.08 s after the TMS pulse in the contralateral (positive cluster, $p = 0.03$) and ipsilesional (negative cluster, $p = 0.006$) hemispheres. A second pair of significant clusters (Fig. 3C–D) emerged in the time interval between 0.13 and 0.19 s after the TMS pulse, in the contralateral (positive cluster; $p = 0.021$) and ipsilesional M1 (negative cluster; $p = 0.004$). This spatial symmetry of the significant clusters is expected as we are comparing non-rectified activity that has been re-referenced against the average of all channels in the preprocessing stage.

In summary, at two time intervals (0.02 to 0.08 s and 0.13 to 0.19 s after TMS pulse) the activity elicited by stimulating the contralateral hemisphere at *trough* is larger in magnitude than the activity elicited by the identical stimulation at *no-trough*. These results confirm the differences that can be appreciated qualitatively in Fig. 2D), at least for the contralateral Hjorth. Crucially, the same statistical contrast comparing the effects of stimulation over iM1 at *trough* vs *no-trough* did not provide any significant result: the smallest cluster p-value in this case is $p = 0.33$.

3.3. Experiment 1 – TFR results

Stimulation at *trough* did not elicit different post-pulse alpha power

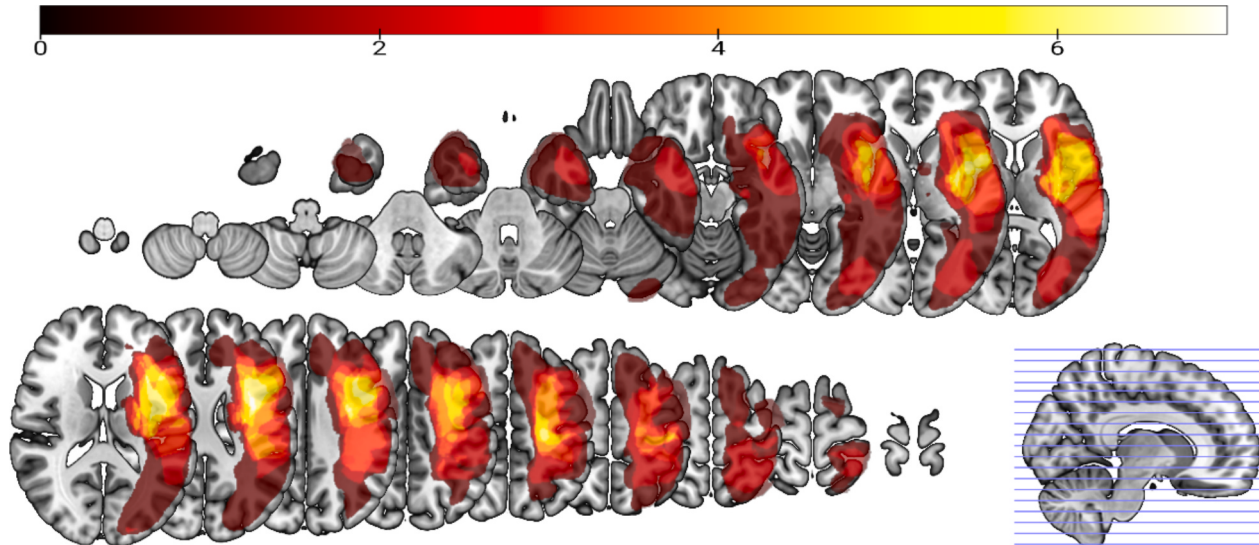


Fig. 1. Radiological view of lesion overlap. 13 out of the 19 patients underwent T1w and/or T2w scans. T1w images were either acquired with clinical sequences or high-resolution research sequences. 6 out of 13 scans from patients with right-hemispheric stroke were flipped to the left side. The maximum overlap (color coded) consists of 7/13 patients. For details on overlap computation, see Supplementary Material.

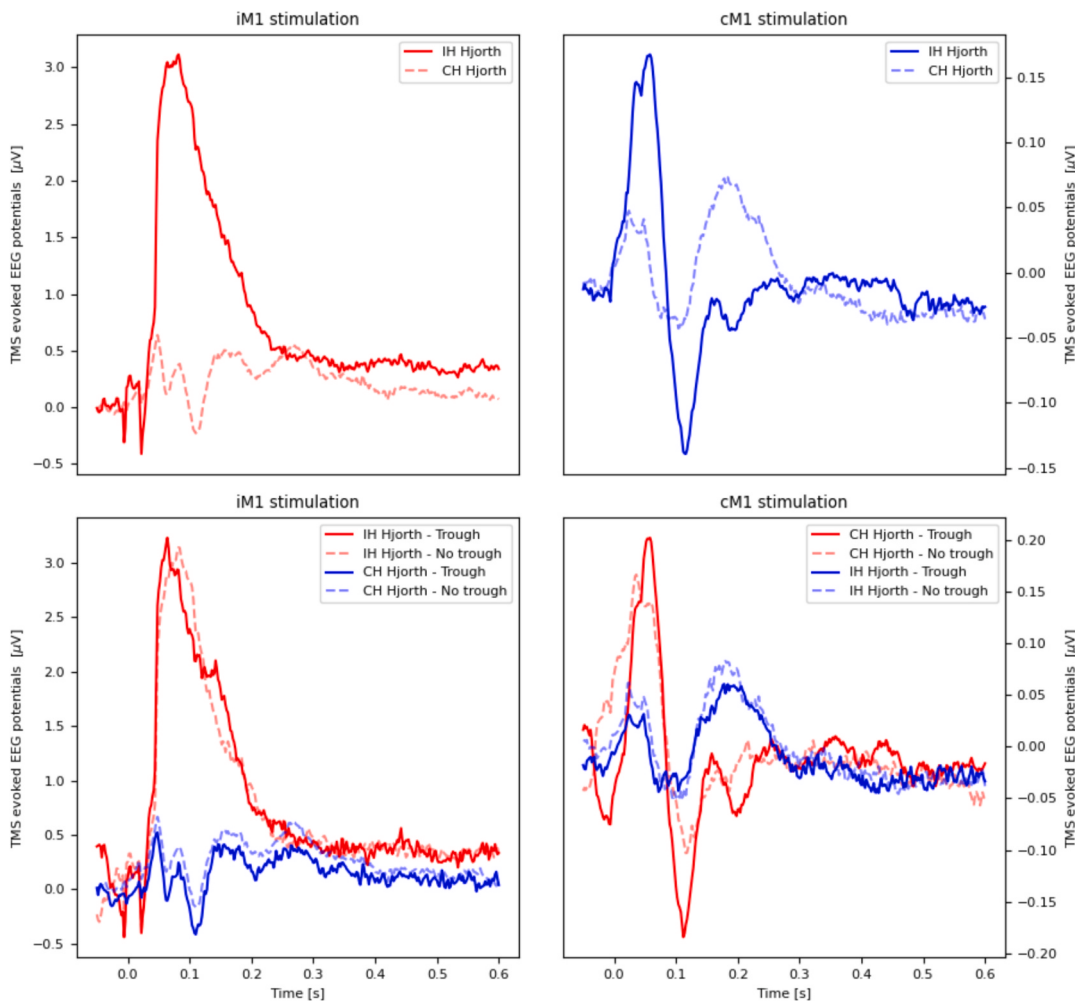


Fig. 2. TEPs with and without post-hoc phase sorting. A) and B) TEPs explored in the ipsilesional (IH) and contralateral hemisphere (CH) without post-hoc phase sorting for A) the stimulation of ipsilesional motor cortex (iM1) and B) the stimulation of contralateral motor cortex (cM1). C and D) TEPs explored in the IH and CH with post-hoc phase sorting (trough vs. no-trough of the ongoing μ -rhythm) for C) ipsilesional M1stimulation of iM1 and D) stimulation of cM1. IH and CH Hjorth EEG recordings refer to C3-centred and C4-centred Hjorth, respectively. All TEPs are grand averages of 12 patients from Experiment 1. Note that the scales on the y-axes are smaller by about one order of magnitude with cM1 stimulation (B, D) compared to iM1 stimulation (A, C), indicating much larger TEPs with iM1 stimulation.

compared to stimulation at *no-trough* for both stimulation of cM1 or iM1. On the contrary, the post-pulse beta power was significantly higher with TMS at *trough* vs. *no-trough* for both cM1 and iM1 (Fig. 4). In particular, we found a significant positive cluster ($p = 0.041$) for stimulation of cM1 in a late period from 0.47 to 0.85 s after the TMS pulse (Fig. 4B) and a longer and earlier positive cluster (from 0.025 to 0.8 s after the TMS pulse; $p = 0.039$) for stimulation of iM1 (Fig. 4A).

Given the nil results in the alpha-band, we performed a sanity check by computing the power spectrum between 5 and 18 Hz of each patient, separately for the ipsilesional and contralateral hemisphere, when applicable. As it can be noticed in Supplementary Fig. 2, the two hemispheres show similar power spectra with regard to IAF.

3.4. Experiment 2 – Degree of excitability differentiation depends on level of impairment

The relationship between the degree of excitability differentiation and the level of motor function (as assessed by the FMA-UE score) was investigated in Experiment 2 (see Fig. 5). The linear fit computed between the individual post-pulse beta power ratio (post-pulse beta power evoked by stimulation of iM1 at *trough* vs. *no-trough*) and the individual FMA-UE score was significant when all channels ($p = 0.022$; $R^2 = 0.304$)

or the right Hjorth channels were used ($p = 0.025$; $R^2 = 0.294$). On the contrary, no significant results were obtained computing the post-pulse beta power over the left Hjorth channels. Differently, the PCI was significantly correlated with the FMA-UE score only when the computation was limited to the left Hjorth channels ($p = 0.025$; $R^2 = 0.291$). No significant correlation was found when the PCI was computed using all channel or the right Hjorth channels. Moreover, the Spearman's rank correlations were significant between the metrics that significantly correlated with the level of impairment. Panels in Fig. 5 report the linear fit plots for the significant metrics, as well as the correlation plots between significant metrics. All the linear fit results, as well as the Spearman's rank correlations between significant metrics, are reported in Table 2.

4. Discussion

This work aimed at evaluating μ -oscillation phase-dependent modulation of TEPs and TFRs when stimulating the ipsilesional or contralateral M1 of chronic stroke patients. To test this, we implemented TEP analyses both with and without (as in (Casula et al., 2021; Tscherpel et al., 2020)) a post-hoc phase bin sorting. The μ -phase-dependent analyses allowed to explore the cortical responses to TMS in greater detail,

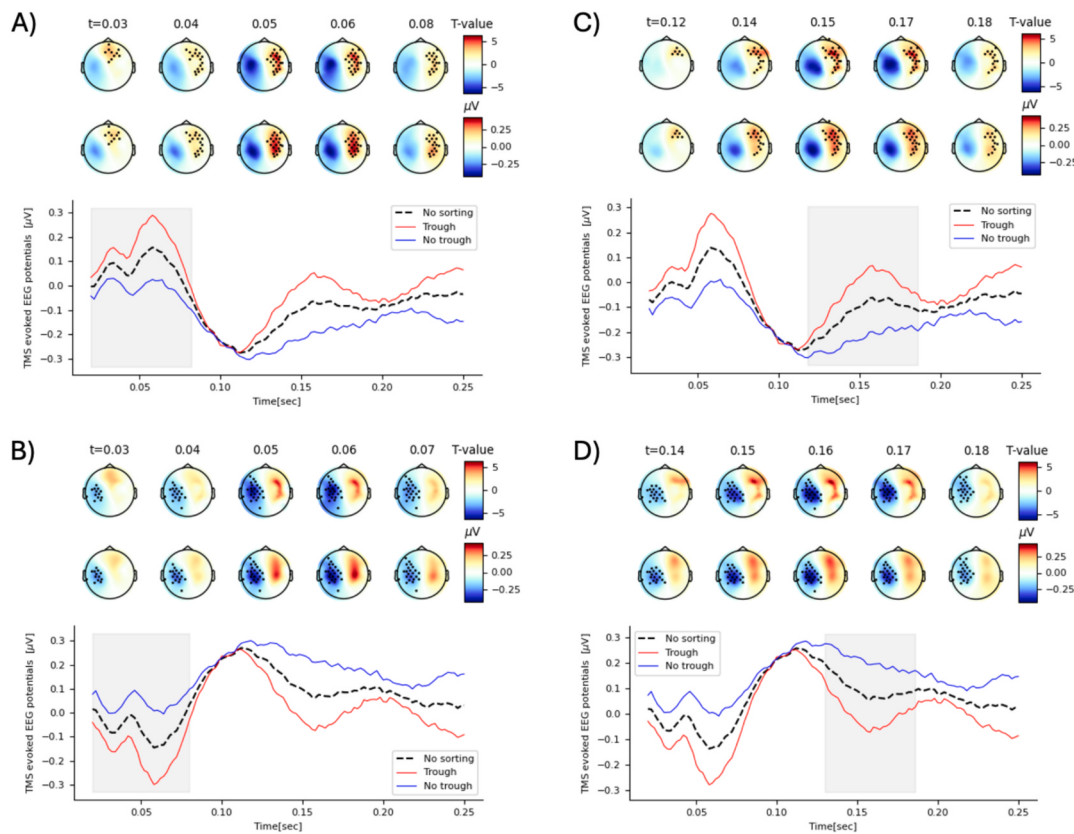


Fig. 3. TEPs evoked by TMS of the contralateral motor cortex, contrasting stimulation during the *trough* vs. *no-trough* of the ongoing μ -rhythm. Each panel show results for a significant cluster (A-B: time interval 0.02–0.08 s; C-D: time interval 0.13–0.19 s). Within each panel, the TEP plots show the TMS-evoked activity averaged over the significant electrodes of the cluster for the *trough* and *no-trough* condition and when no phase sorting is used. The topoplots rows show the topographic distribution of the T-values (top row) and the TMS evoked activity difference between the two contrasted phase conditions (in μ V, bottom row), averaged across time windows within the significant cluster epochs. Dots in the topoplots correspond to significant electrodes belonging to the cluster. Periods of significant differences between *trough* vs. *no-trough* condition are indicated by the shaded gray area. Time is in seconds after the TMS pulse.

compared to the standard analyses. The only appreciable difference between TMS of ipsilesional vs. contralateral M1 without phase-sorting was a large and low-complexity response when stimulating the ipsilesional M1 (Fig. 2A). This finding in our moderately-to-severely impaired patient group confirms previous reports in patients with comparable motor impairment (Harquel et al., 2022; Sarasso et al., 2020; Tecchio et al., 2023; Tscherpel et al., 2020; Tscherpel et al., 2024) but not in less affected patients (Casula et al., 2021).

Further studies have provided rather inconsistent TMS-EEG stroke signatures for recovery: Pellicciari et al. evaluated stroke patients with TMS-EEG at three different time points during recovery (40, 60 and 180 days after stroke, respectively) (Pellicciari et al., 2018). They found that increased alpha oscillation power correlated with recovery, proposing this metric for successful rehabilitation. Recently, Bai et al. reported an amplitude reduction of the N100 TEP component in the ipsilesional M1, as well as poor intra- and interhemispheric theta connectivity in the ipsilesional M1 compared to the contralateral one (Bai et al., 2023). They concluded that the N100 potential can be considered a useful biomarker for recovery. Finally, Ding et al. found increased intra-hemispheric functional connectivity to be beneficial for rehabilitation in well-recovering severe stroke patients without MEPs (Ding et al., 2023). Conversely, in less severe patients with MEPs the opposite relationship between functional connectivity and successful recovery was reported.

Given this scattered picture, we tried to clarify a possible source of variability of TMS-EEG responses in stroke by post-hoc sorting TEPs and TFRs on the basis of instantaneous μ -phase at the time of single-pulse TMS. In line with previous findings in healthy subjects (Desideri et al.,

2019), stimulation of the contralateral M1 at the *trough* elicited larger TEPs in both the stimulated contralateral hemisphere and in the ipsilesional M1 contralateral to stimulation, compared to stimulation at *no-trough* (Fig. 2C). This result is in accordance with the notion that the *trough* of the μ -oscillation reflects a state of high sensorimotor cortical excitability (Zrenner et al., 2018) and that the amplitude of TEPs is a marker of cortical excitability at the time of stimulation (Desideri et al., 2019; Gordon et al., 2022). The observation that contralateral M1 stimulation elicits larger TEPs at *trough* vs. *no-trough*, in both the stimulated contralateral and non-stimulated ipsilesional M1, suggests that the differentiation of μ -phase-dependent excitability states is preserved within contralateral M1 in moderate-to-severe chronic stroke patients.

In contrast, TMS of the ipsilesional M1 shows relevantly less differentiation in TEP amplitude in the *trough* vs. *no-trough* condition in both the stimulated ipsilesional M1 and non-stimulated contralateral hemisphere (Fig. 2B). In fact, the statistical test comparing TEPs evoked in the two different phase-states showed no significant difference in the TEPs amplitudes.

This preserved differentiation of excitability states in the contralateral M1 was partially confirmed by the TFR analysis. Previous work has shown that post-pulse power modulation occurs both in the alpha and beta bands after single-pulse TMS in healthy participants (e.g., Fecchio et al., 2017; Manganotti et al., 2012). Additionally, studies have demonstrated that post-pulse alpha and beta power modulation is influenced by rTMS and continuous theta burst (cTBS) interventions, suggesting their potential as markers of cortical excitability (e.g., Chung et al., 2015; Veniero et al., 2011; Vernet et al., 2013). In light of findings that the phase of the μ -rhythm modulates M1 excitability (Zrenner et al.,

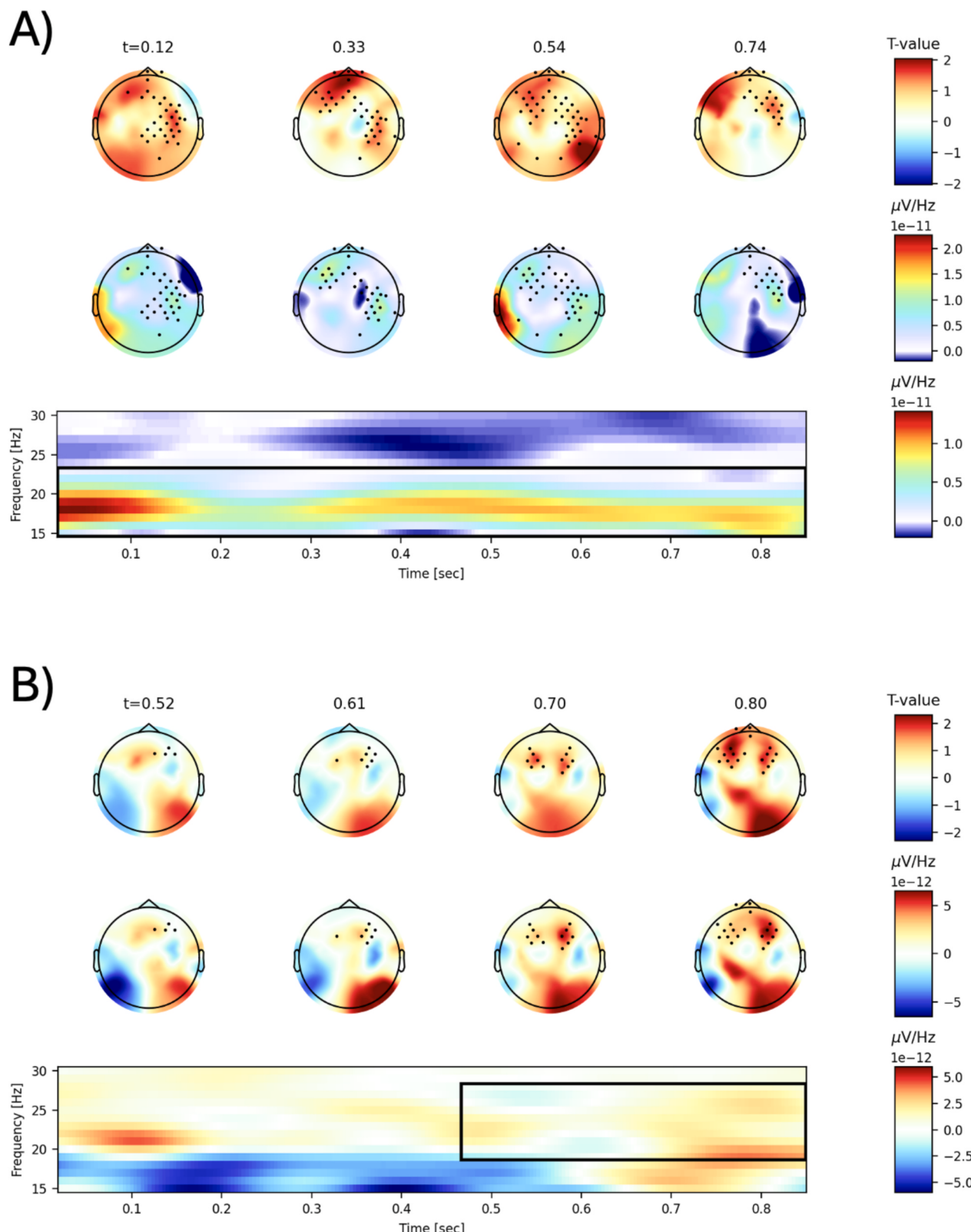


Fig. 4. Cluster statistics on TFRs after ipsilesional and contralateral M1 stimulation in the beta-frequency band. Significant clusters for the TMS-evoked power in the beta band for stimulation of iM1 (A) and stimulation of cM1 (B). Each panel summarizes the results of the statistical analysis. In the bottom plot the difference between the TMS-evoked power in the *trough* vs. *no-trough* condition is shown. The black square highlights the significant cluster extension. The topoplots rows show the topographic distribution of the T-values (top row) and the TMS-evoked power difference (bottom row), averaged across time and frequency within the significant cluster. Dots in the topoplots correspond to significant electrodes belonging to the cluster. Time is in seconds after the TMS pulse.

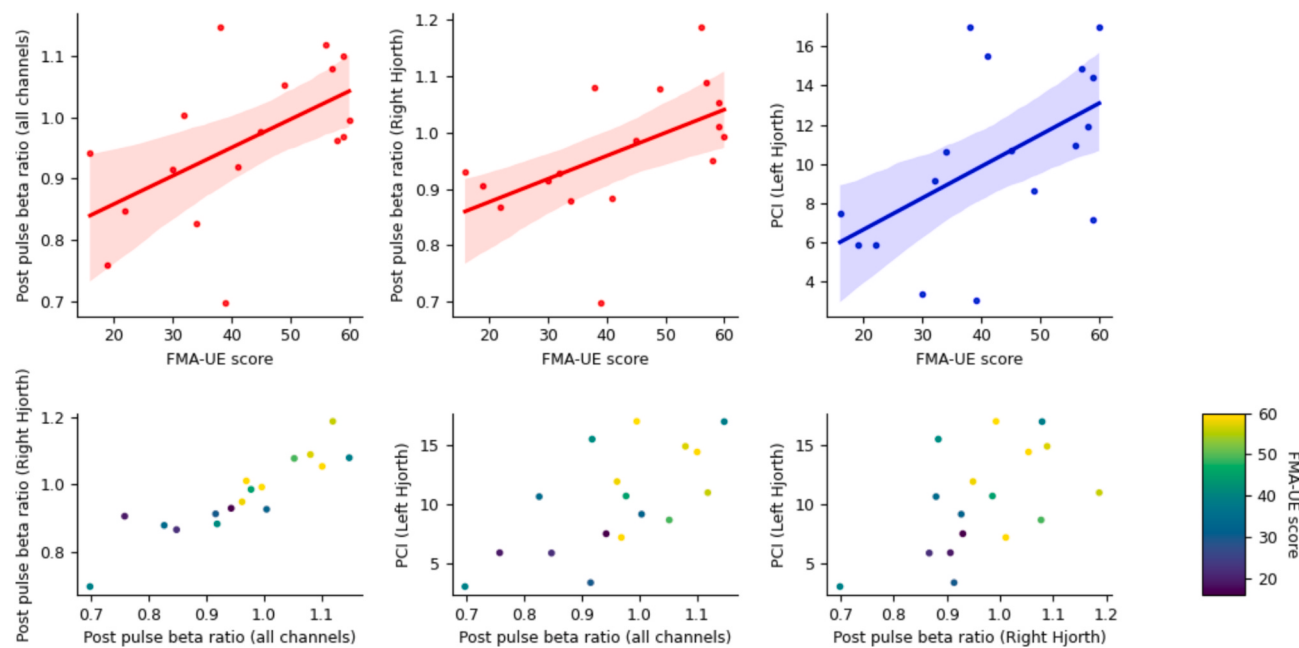


Fig. 5. Post-pulse beta power ratio and PCI regressions against FMA-UE score with TMS of ipsilesional motor cortex. **Top row)** Scatter plots of significant metrics against FMA-UE score. The solid line represent the linear fit with 95% confidence intervals. For each plot, y-axes labels indicate the correspondent metrics. **Bottom row)** Correlation between the different significant metrics. The axes labels indicate the correspondent metrics. Each dot is color coded according to the FMA-UE score. In all plots, each data point corresponds to one stroke patient in Experiment 2.

Table 2

Correlation results for the metrics in Experiment 2. **Diagonal cells)** Results of linear fits between the post-pulse beta ratio and the PCI against FMA-UE score, for the different selection of channels as outlined in the main text. Each cell reports the p-value for the slope of the linear model and the R-squared, indicating the amount of variance explained by the model. **Off diagonal cells)** Spearman's rank correlation test results between all the metrics. Non-significant results are reported in gray text.

		Post pulse beta power ratio			Perturbation Complexity Index		
		All channels	Right Hjorth	Left Hjorth	All channels	Right Hjorth	Left Hjorth
Post pulse beta power ratio	All channels	p = 0.022 R ² = 0.304					
	Right Hjorth	p = 2 x 10 ⁻⁷	p = 0.025 R ² = 0.294				
	Left Hjorth	p = 0.003	p = 0.005	p = 0.45 R ² = 0.04			
Perturbation Complexity Index	All channels	p = 0.17	p = 0.66	p = 0.53	p = 0.31 R ² = 0.07		
	Right Hjorth	p = 0.25	p = 0.67	p = 0.59	p = 0.013	p = 0.45 R ² = 0.04	
	Left Hjorth	p = 0.004	p = 0.02	p = 0.19	p = 0.07	p = 0.02	p = 0.025 R ² = 0.291

2018), we hypothesized larger *trough* vs. *no-trough* post-pulse alpha and beta power if the differentiation between excitability states was preserved. Our results revealed no evidence of phase-dependent modulation in post-pulse alpha power in either the contralateral or ipsilesional hemisphere. By contrast, post-pulse beta power was clearly modulated by the phase of the μ -rhythm, showing significantly higher power after stimulation at the *trough* compared to *no-trough* in both hemispheres, with modulation being stronger in the ipsilesional M1. These findings are in line with the consistent relationship between beta-band activity and motor cortical excitability, and its established role in motor control and cortico-muscular communication in stroke patients (Foong et al., 2019; Wu et al., 2016). The stronger link of beta power with cortical excitability modulation may reflect its localized and specific role in the motor cortex. As noted by Veniero et al. (2011), beta-band synchronization is tightly linked to cortico-muscular communication and is primarily localized to the motor cortex, aligning with its role in regulating excitability states relevant to motor function. This functional specificity may explain why beta activity, compared to alpha, showed a clearer

phase-dependent modulation in both hemispheres.

In Experiment 2, we observed that the level of excitability differentiation correlated with motor function in the affected upper extremity. In line with our hypothesis, we found the degree of ipsilesional motor cortical excitability differentiation (as expressed by the post-pulse beta power evoked by stimulation of ipsilesional M1 at *trough* vs. *no-trough*), correlated with the individual FMA-UE score (Fig. 5A). The degree of differentiation reflected in the post-pulse beta power ratio is in line with previous literature, in which correlations between beta power and motor performance in stroke patients have been reported (e.g., (Foong et al., 2019, Wu et al., 2016)).

Our results are consistent with the idea that the low degree of excitability differentiation in ipsilesional M1 in chronic stroke patients reflects a dysregulation of the μ -rhythm activity in sharpening the neural recruitment within the sensorimotor system. In this regard, our findings on the μ -phase-dependent modulation of M1 excitability (previously reported in healthy participants by (Baur et al., 2020, Desideri et al., 2019, Wischnewski et al., 2022, Zrenner et al., 2022, Zrenner et al.,

2018, Suresh and Hussain, 2023; Zrenner et al., 2023) in the contralateral M1 of chronic stroke patients is in line with previous findings from intracranial recordings in the somatosensory cortex of monkeys showing that alpha oscillations exhibit a rhythmic relation with neuronal spiking, such that firing is highest at the trough of the local field potential alpha oscillation (Haegens et al., 2011). Since surround inhibition is implicated in the sharpening of neural recruitment (Blakemore and Cooper, 1970), a dysregulation in this mechanism could potentially result in increased neural recruitment that may explain the increased TEP amplitude following stimulation of the ipsilesional M1. Of note, similarly increased and low-complexity TEPs are also found in typically developing children (Määttä et al., 2017) in whom surround inhibition mechanisms are not fully developed when compared to adults (Säisänen et al., 2018). Our results in Experiment 1 show differences in TEP amplitudes depending on the local μ -rhythm state after stimulation of the contralateral but not ipsilesional M1. In particular, the low excitability state (*no-trough* condition) elicited lower TEP amplitudes, with respect to the *trough* condition, with stimulation of the contralateral M1 (Fig. 2D). The same does not occur in the ipsilesional M1, where TEP amplitudes were comparable in the *trough* vs. *no-trough* condition (Fig. 2C). Crucially, TEPs evoked at *no-trough* (the low-excitability state) in the ipsilesional M1 showed greater amplitude with respect to the TEPs evoked at *no-trough* in the contralateral hemisphere. We argue that the lower excitability differentiation in the ipsilesional M1 might provide new insights on the observed (in this study as well as in (Sarasso et al., 2020, Tecchio et al., 2023, Tscherpel et al., 2020)) exaggerated response to TMS of ipsilesional M1, compared to stimulation of contralateral M1 and healthy controls.

Experiment 2 further suggests that a fingerprint of severely affected stroke patients may be a lack of restoration of a functional differentiation between the local excitability states of the ipsilesional M1. Crucially, we also show here that this loss in differentiation between the excitability states is only partially related to the PCI (see Fig. 5 and Table 2), a measure of the algorithmic complexity of the spatio-temporal EEG response to TMS (Casali et al., 2013). Differently from the post-pulse beta ratio, the PCI did not correlate with FMA-UE when computed on all channels, but only when the local activity was considered. Moreover, the amount of variance explained by the linear fit of the post-pulse beta ratio computed on all channels was larger than the one from the PCI when a restricted number of channels were selected. This suggests that the correlation of these metrics with the level of impairment cannot be completely explained by a simple loss of complexity and that the post-pulse beta ratio is a potential candidate for a better and more general marker of recovery.

5. Limitations

The sample size is small (12 patients in Experiment 1, 17 patients in Experiment 2) but both, difficulty in testing stroke populations in extensive TMS Experiments, and physiological constraints of post-hoc subdivision of the phase-dependent TMS effects contributed to the limited sample size. Our findings will require replication in larger independent patient cohorts. Another limitation is that the lesion location was not taken into account in the analysis. The inclusion criterion of preserved MEPs in the paretic hand when stimulating the ipsilesional M1 indicates an at least partially intact M1 and corticospinal tract, but Fig. 1 shows substantial variability in location and size of lesions that may have affected the results. We acknowledge that stimulating above the MEP threshold (115 % RMT) may introduce reaferference of somatosensory information, particularly when stimulating the contralateral hemisphere, as highlighted in previous studies (Petrichella et al., 2017, Tecchio et al., 2017). This reaferference could influence the spectral features of the EEG response and should be considered when interpreting the results.

6. Conclusions

In this work, we have shown that the differentiation between μ -oscillation-dependent excitability states of the ipsilesional M1 is a peculiar feature of degradation in chronic stroke patients that is significantly related to the level of motor impairment as measured by the FMA-UE. These findings suggest that this degree of differentiation, especially the metric of the post-pulse beta power ratio, could be potentially used as a biomarker for motor stroke severity and its incomplete recovery in chronic stroke. This can be of particular interest in clinical practice, since TMS-evoked EEG potentials, differently from MEPs, are measurable in virtually all stroke patients. Further investigation in longitudinal studies is required in this direction to understand how the degree of excitability differentiation and, in particular, the post-pulse beta power develops over time and to what extent it predicts the capacity for motor stroke recovery.

Competing interests

U.Z. received grants from the European Research Council (ERC), German Ministry of Education and Research (BMBF), German Research Foundation (DFG), and consulting fees from CorTec GmbH. Other authors report no competing interests.

CRediT authorship contribution statement

Arianna Brancaccio: Conceptualization, Methodology, Software, Formal analysis, Data curation, Writing – original draft, Writing – review & editing, Visualization. **Davide Tabarelli:** Methodology, Software, Writing – review & editing. **David Baur:** Investigation, Data curation, Writing – original draft, Writing – review & editing. **Johanna Roesch:** Investigation, Writing – review & editing. **Wala Mahmoud:** Investigation, Writing – review & editing. **Ulf Ziemann:** Resources, Supervision, Writing – original draft, Writing – review & editing. **Paolo Belardinelli:** Resources, Supervision, Writing – original draft, Writing – review & editing.

Acknowledgements/Funding

UZ has received funding from the European Research Council (ERC Synergy) under the European Union's Horizon 2020 research and innovation programme (ConnectToBrain; grant agreement No 810377).

Data availability

Public sharing of raw data is not possible due to the data protection agreement with the participants. Preprocessed and fully deidentified data can be made available upon reasonable request directed to the corresponding author.

Appendix A. Supplementary material

Supplementary data to this article can be found online at <https://doi.org/10.1016/j.clinph.2025.2110747>.

References

- Bai, Z., Zhang, J.J., Fong, K.N., 2023. Intracortical and intercortical networks in patients after stroke: a concurrent TMS-EEG study. *J. Neuroeng. Rehabil.* 20 (1), 100.
- Baur, D., Galevska, D., Hussain, S., Cohen, L.G., Ziemann, U., Zrenner, C., 2020. Induction of LTD-like corticospinal plasticity by low-frequency rTMS depends on pre-stimulus phase of sensorimotor μ -rhythm. *Brain Stimul.* 13 (6), 1580–1587.
- Belardinelli, P., König, F., Liang, C., Premoli, I., Desideri, D., Müller-Dahlhaus, F., et al., 2021. TMS-EEG signatures of glutamatergic neurotransmission in human cortex. *Sci. Rep.* 11 (1), 8159.
- Blakemore, C., Cooper, G.F., 1970. Development of the brain depends on the visual environment. *Nature* 228 (5270), 477–478.

- Brainin, M., Teuschl, Y., Kalra, L., 2007. Acute treatment and long-term management of stroke in developing countries. *Lancet Neurol.* 6 (6), 553–561.
- Casali, A.G., Gosseries, O., Rosanova, M., Boly, M., Sarasso, S., Casali, K.R., et al., 2013. A theoretically based index of consciousness independent of sensory processing and behavior. *Sci. Transl. Med.* 5 (198), 198ra05.
- Casula, E.P., Pellicciari, M.C., Bonni, S., Spanò, B., Ponzo, V., Salsano, I., et al., 2021. Evidence for interhemispheric imbalance in stroke patients as revealed by combining transcranial magnetic stimulation and electroencephalography. *Hum. Brain Mapp.* 42 (5), 1343–1358.
- Casula, E.P., Tarantino, V., Bassi, D., Arcara, G., Marino, G., Toffolo, G.M., et al., 2014. Low-frequency rTMS inhibitory effects in the primary motor cortex: Insights from TMS-evoked potentials. *Neuroimage* 98, 225–232.
- Chung, S.W., Rogasch, N.C., Hoy, K.E., Fitzgerald, P.B., 2015. Measuring brain stimulation induced changes in cortical properties using TMS-EEG. *Brain Stimul.* 8 (6), 1010–1020.
- Comolatti, R., Pigorini, A., Casarotto, S., Fecchio, M., Faria, G., Sarasso, S., et al., 2019. A fast and general method to empirically estimate the complexity of brain responses to transcranial and intracranial stimulations. *Brain Stimul.* 12 (5), 1280–1289.
- Darmani, G., Zips, C.M., Böhmer, G.M., Deschet, K., Müller-Dahlhaus, F., Belardinelli, P., et al., 2016. Effects of the selective α5-GABAAR antagonist S44819 on excitability in the human brain: a TMS-EMG and TMS-EEG phase I study. *J. Neurosci.* 36 (49), 12312–12320.
- Delorme, A., Makeig, S., 2004. EEGLAB: an open source toolbox for analysis of single-trial EEG dynamics including independent component analysis. *J. Neurosci. Methods* 134 (1), 9–21.
- Desideri, D., Zrenner, C., Gordon, P.C., Zieman, U., Belardinelli, P., 2018. Nil effects of μ-rhythm phase-dependent burst-rTMS on cortical excitability in humans: a resting-state EEG and TMS-EEG study. *PLoS One* 13 (12), e0208747.
- Desideri, D., Zrenner, C., Zieman, U., Belardinelli, P., 2019. Phase of sensorimotor μ-oscillation modulates cortical responses to transcranial magnetic stimulation of the human motor cortex. *J. Physiol.* 597 (23), 5671–5686.
- Ding, Q., Chen, J., Zhang, S., Chen, S., Li, X., Peng, Y., et al., 2023. Neurophysiological characterization of stroke recovery: a longitudinal TMS and EEG study. *CNS Neurosci. Ther.*
- Fecchio, M., Pigorini, A., Comanducci, A., Sarasso, S., Casarotto, S., Premoli, I., et al., 2017. The spectral features of EEG responses to transcranial magnetic stimulation of the primary motor cortex depend on the amplitude of the motor evoked potentials. *PLoS One* 12 (9), e0184910.
- Foong, R., Ang, K.K., Quek, C., Guan, C., Phua, K.S., Kuah, C.W.K., et al., 2019. Assessment of the efficacy of EEG-based MI-BCI with visual feedback and EEG correlates of mental fatigue for upper-limb stroke rehabilitation. *IEEE Trans. Biomed. Eng.* 67 (3), 786–795.
- Fugl-Meyer, A.R., Jaasko, L., Leyman, I., Olsson, S., Steglind, S., 1975. The post-stroke hemiplegic patient. 1. A method for evaluation of physical performance. *Scand. J. Rehabil. Med.* 7 (1), 13–31.
- Gordon, P.C., Belardinelli, P., Stenroos, M., Zieman, U., Zrenner, C., 2022. Prefrontal theta phase-dependent rTMS-induced plasticity of cortical and behavioral responses in human cortex. *Brain Stimul.* 15 (2), 391–402.
- Gramfort, A., Luessi, M., Larson, E., Engemann, D.A., Strohmeier, D., Brodbeck, C., Goj, R., Jas, M., Brooks, T., Parkkonen, L., Hämäläinen, M., 2013. MEG and EEG data analysis with MNE-Python. *Front. Neurosci.* 7 (267), 1–13.
- Haegens, S., Nácher, V., Luna, R., Romo, R., Jensen, O., 2011. α-Oscillations in the monkey sensorimotor network influence discrimination performance by rhythmical inhibition of neuronal spiking. *Proc. Natl. Acad. Sci.* 108 (48), 19377–19382.
- Harquel, S., Cadic-Melchior, A., Morishita, T., Fleury, L., Witon, A., Ceroni, M., et al., 2022. Stroke recovery-related changes in cortical reactivity based on modulation of intracortical inhibition. *Stroke.*
- Harris, C.R., Millman, K.J., van der Walt, S.J., et al., 2020. Array programming with NumPy. *Nature* 585, 357–362.
- Hussain, S.J., Hayward, W., Fourcand, F., Zrenner, C., Zieman, U., Buch, E.R., et al., 2020. Phase-dependent transcranial magnetic stimulation of the lesioned hemisphere is accurate after stroke. *Brain Stimul.: Basic, Trans. Clin. Res. Neuromodulation* 13 (5), 1354–1357.
- Katan, M., Luft, A., 2018. Global burden of stroke. *Seminars in neurology.* Thieme Medical Publishers 208–211.
- Määttä, S., Könönen, M., Kallionemi, E., Lakka, T., Lintu, N., Lindi, V., et al., 2017. Development of cortical motor circuits between childhood and adulthood: a navigated TMS-HdEEG study. *Hum. Brain Mapp.* 38 (5), 2599–2615.
- Manganotti, P., Formaggio, E., Storti, S.F., De Massari, D., Zamboni, A., Bertoldo, A., et al., 2012. Time-frequency analysis of short-lasting modulation of EEG induced by intracortical and transcallosal paired TMS over motor areas. *J. Neurophysiol.* 107 (9), 2475–2484.
- Maris, E., Oostenveld, R., 2007. Nonparametric statistical testing of EEG-and MEG-data. *J. Neurosci. Methods* 164 (1), 177–190.
- Mutanen, T.P., Kukkonen, M., Nieminen, J.O., Stenroos, M., Sarvas, J., Ilmoniemi, R.J., 2016. Recovering TMS-evoked EEG responses masked by muscle artifacts. *Neuroimage* 139, 157–166.
- Mutanen, T.P., Metsomaa, J., Liljander, S., Ilmoniemi, R.J., 2018. Automatic and robust noise suppression in EEG and MEG: The SOUND algorithm. *Neuroimage* 166, 135–151.
- Pellicciari, M.C., Bonni, S., Ponzo, V., Cinnella, A.M., Mancini, M., Casula, E.P., et al., 2018. Dynamic reorganization of TMS-evoked activity in subcortical stroke patients. *Neuroimage* 175, 365–378.
- Petrichella, S., Johnson, N., He, B., 2017. The influence of corticospinal activity on TMS-evoked activity and connectivity in healthy subjects: a TMS-EEG study. *PLoS One* 12 (4), e0174879.
- Premoli, I., Castellanos, N., Rivolta, D., Belardinelli, P., Bajo, R., Zipser, C., et al., 2014. TMS-EEG signatures of GABAergic neurotransmission in the human cortex. *J. Neurosci.* 34 (16), 5603–5612.
- Rogasch, N.C., Thomson, R.H., Farzan, F., Fitzgibbon, B.M., Bailey, N.W., Hernandez-Pavon, J.C., et al., 2014. Removing artefacts from TMS-EEG recordings using independent component analysis: importance for assessing prefrontal and motor cortex network properties. *Neuroimage* 101, 425–439.
- Rossi, S., Antal, A., Bestmann, S., Bikson, M., Brewer, C., Brockmöller, J., Carpenter, L.L., Cincotta, M., Chen, R., Daskalakis, J.D., Di Lazzaro, V., Fox, M.D., George, M.S., Gilbert, D., Kimiskidis, V.K., Koch, G., Ilmoniemi, R.J., Pascal Lefèuvre, J., Leocani, L., Lisanby, S.H., Miniusi, C., Padberg, F., Pascual-Leone, A., Paulus, W., Peterchev, A.V., Quartarone, A., Rotenberg, A., Rothwell, J., Rossini, P.M., Santarnecchi, E., Shafai, M.M., Siebner, H.R., Ugawa, Y., Wassermann, E.M., Zangen, A., Zieman, U., Hallett, M., 2021. Safety and recommendations for TMS use in healthy subjects and patient populations, with updates on training, ethical and regulatory issues: expert guidelines. *Clin. Neurophysiol.* 132 (1), 269–306.
- Rossini, P.M., Burke, D., Chen, R., Cohen, L.G., Daskalakis, Z., Di Iorio, R., Di Lazzaro, V., Ferreri, F., Fitzgerald, P.B., George, M.S., Hallett, M., Lefèuvre, J.P., Langguth, B., Matsumoto, H., Miniusi, C., Nitsche, M.A., Pascual-Leone, A., Paulus, W., Rossi, S., Rothwell, J.C., Siebner, H.R., Ugawa, Y., Walsh, V., Zieman, U., 2015. Non-invasive electrical and magnetic stimulation of the brain, spinal cord, roots and peripheral nerves: Basic principles and procedures for routine clinical and research application. An updated report from an IFCN Committee. *Clin. Neurophysiol.* 126 (6), 1071–1107.
- Säisänen, L., Julkunen, P., Lakka, T., Lindi, V., Könönen, M., Määttä, S., 2018. Development of corticospinal motor excitability and cortical silent period from mid-childhood to adulthood—a navigated TMS study. *Neurophysiol. Clin.* 48 (2), 65–75.
- Sarasso, S., D'Ambrosio, S., Fecchio, M., Casarotto, S., Viganò, A., Landi, C., et al., 2020. Local sleep-like cortical reactivity in the awake brain after focal injury. *Brain* 143 (12), 3672–3684.
- Suresh, T., Hussain, S.J., 2023. Re-evaluating the contribution of sensorimotor mu rhythm phase and power to human corticospinal output: a replication study. *Brain Stimul.* 16, 936–938.
- Tallon-Baudry, C., Bertrand, O., Delpuech, C., Pernier, J., 1997. Oscillatory gamma-band (30–70 Hz) activity induced by a visual search task in humans. *J. Neurosci.* 722–734.
- Tecchio, F., Giambattistelli, F., Porcaro, C., Cottone, C., Mutanen, T.P., Pizzella, V., et al., 2023. Effective intracerebral connectivity in acute stroke: a TMS-EEG study. *Brain Sci.* 13 (2), 233.
- Tscherpel, C., Dern, S., Hensel, L., Zieman, U., Fink, G.R., Grefkes, C., 2020. Brain responsiveness provides an individual readout for motor recovery after stroke. *Brain* 143 (6), 1873–1888.
- Tscherpel, C., Mustin, M., Massimini, M., Paul, T., Zieman, U., Fink, G.R., et al., 2024. Local Neuronal Sleep after Stroke: The role of cortical bistability in brain reorganization. *Brain Stimul.* 17, 836–846.
- Veniero, D., Brignani, D., Thut, G., Miniusi, C., 2011. Alpha-generation as basic response-signature to transcranial magnetic stimulation (TMS) targeting the human resting motor cortex: a TMS/EEG co-registration study. *Psychophysiology* 48 (10), 1381–1389.
- Vernet, M., Bashir, S., Yoo, W.K., Perez, J.M., Najib, U., Pascual-Leone, A., 2013. Insights on the neural basis of motor plasticity induced by theta burst stimulation from TMS-EEG. *Eur. J. Neurosci.* 37 (4), 598–606.
- Virtanen, P., et al., 2020. SciPy 1.0: fundamental algorithms for scientific computing in Python. *Nat. Methods* 17 (3), 261–272.
- Wischnewski, M., Haigh, Z.J., Shirinpour, S., Alekseichuk, I., Opitz, A., 2022. The phase of sensorimotor mu and beta oscillations has the opposite effect on corticospinal excitability. *Brain Stimul.* 15 (5), 1093–1100.
- Wu, J., Srinivasan, R., Burke Quinlan, E., Solodkin, A., Small, S.L., Cramer, S.C., 2016. Utility of EEG measures of brain function in patients with acute stroke. *J. Neurophysiol.* 115 (5), 2399–2405.
- Zrenner, C., Belardinelli, P., Ermolova, M., Gordon, P.C., Stenroos, M., Zrenner, B., et al., 2022. μ-rhythm phase from somatosensory but not motor cortex correlates with corticospinal excitability in EEG-triggered TMS. *J. Neurosci. Methods* 379, 109662.
- Zrenner, C., Desideri, D., Belardinelli, P., Zieman, U., 2018. Real-time EEG-defined excitability states determine efficacy of TMS-induced plasticity in human motor cortex. *Brain Stimul.* 11 (2), 374–389.
- Zrenner, C., Kozák, G., Schaworowkow, N., Metsomaa, J., Baur, D., Vetter, D., et al., 2023. Corticospinal excitability is highest at the early rising phase of sensorimotor μ-rhythm. *Neuroimage* 266, 119805.